THE JOURNAL OF PHYSICAL CHEMISTRY B

Article

pubs.acs.org/JPCB

Soybean Oleosomes Behavior at the Air−Water Interface

Gustav Waschatko,[†,‡,*] Birgitta Schiedt,[†] Thomas A. Vilgis,[†] and Ann Junghans[†]

[†]Max Planck Institute for Polymer Research, Ackermannweg 10, 55128 Mainz, Germany

[‡]Institut für Pharmazie und Biochemie, Johannes Gutenberg Universität Mainz, Johann-Joachim-Becher-Weg 30, 55128 Mainz, Germany

Web-Enhanced Feature

ABSTRACT: Soy milk is a highly stable emulsion, the stability being mainly due to the presence of oleosomes or oil bodies, spherical structures filled with triacylglycerides (TAGs) and surrounded by a monolayer of phospholipids and proteins called oleosins. For oleosomes purified from raw soymilk, surface pressure investigations and Brewster angle microscopy have been performed to unveil their adsorption, rupture and structural changes over time at different subphase conditions (pH, ionic strength). Such investigations are important for (industrial) food applications of oleosomes, but are also useful for the understanding of the general behavior of proteins and phospholipids at interfaces. In addition a better comprehension of the highly stable oleosomes can lead to advancements in liposome manufacturing, e.g., for storage and transport applications. Although oleosomes have their origin in food systems, their unique stability and physical behavior show transferable characteristics which lead to a much better understanding of the description of any kind of emulsion. This study is one of the first steps toward the comparison of natural emulsification concepts based on different physical structures: e.g., the animals' low density lipoproteins, where apolipoproteins with phospholipids are located only at the interface and plant oleosomes with its oleosins, which are embedded in a phospholipid monolayer and reach deep inside the oil phase.

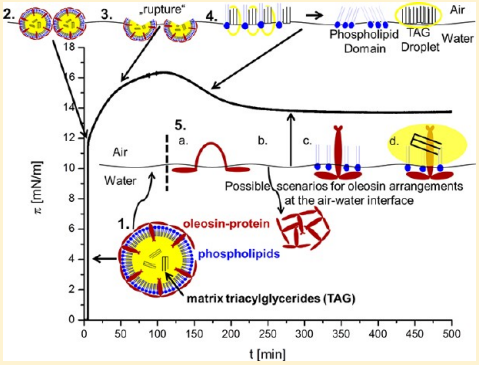

INTRODUCTION

Emulsions, e.g., mixtures of typically immiscible liquids such as water and triacylglycerides, contain stable droplets of oil immersed in water, which are stabilized by emulsifiers. "Classical" emulsifiers are based on the interface activity of their hydrophilic and hydrophobic (lipophilic) part. Obviously, this arrangement and their polarity define their emulsifying capacity usually expressed by the HLB (hydrophilic−lipophilic balance) value.[1] The charge of the hydrophilic part depends on the pH-value and the ionic strength of the solution, which thereby defines the stability of the emulsion. Of course, the nature of the emulsifying process is determined by the architecture of the surface active molecules. Whereas in phospholipid stabilized systems, a simple head−tail structure is sufficient, emulsifying proteins need a certain primary structure to produce a relevant surface activity (see, for example, refs 2−4). Although nature has a limited amount of natural emulsifiers, i.e., phospholipids and proteins, evolution has developed different native structures to solubilize oil in water via small droplets: in animals lipoproteins (HDL = high-density lipoprotein, LDL = low-density lipoprotein, chylomicrometers), in milk lipid or fat globules, in plants oleosomes or oil bodies (OB).[5−7] For example, on closer examination the lipid droplets produced in animals are completely different with regards to their surface proteins than plant oleosomes. One very high mass apolipoprotein, e.g., hen apolipoprotein B (UniProtKB: Q197x2) in egg yolk, with its 4631 amino acids wound around the whole particle, is located more or less close to the surface made of phospholipids.[8,9] Thus, it significantly constrains the dynamics of the phospholipids in the domains close to the proteins. The benefit of the apolipoproteins is therefore obvious; they yield more stable droplets than "classical" emulsions where only phospholipids are used.

Nevertheless, oleosomes appear even more stable than LDL-particles, for example from egg yolk. The reason is a different arrangement of stabilizing proteins. Basically, oleosomes can be viewed as micelle-like structures with an outer phospholipid monolayer, an interior filled with TAGs (triacylglycerides), and associated proteins, the so-called oleosins (Figure 7).[7] Oleosins are alkaline proteins of 15−30 kDa expressed during seed development and maturation and presumably play a major role in the stability of oil bodies.[10] In contrast to the apolipoproteins in LDL particles these oleosins are not just located on the surface but are most likely anchored with their central hydrophobic stretch deep in the oil-phase (Figure 7). This assumption regarding the location of the hydrophobic domain, as well as the existence of a prolin knot forming a 180° turn of a "hairpin"-like sequence, are commonly accepted.[11] However, the secondary structure of the longest hydrophobic sequence known to date (about 70 amino acids) is not yet fully determined and is debated to be either antiparallel β-strands[12] or α-helical[13]. The N- and C-terminal domains are more

Received: December 9, 2011
Revised: July 20, 2012
Published: July 23, 2012

hydrophilic (e.g., amphipathic α-helix[10]), most probably remain umbrella-like outside of the oleosome, and are less conserved among plant species. The physics of the oil bodies is relatively complicated. In soybeans there are four oleosins with evidence at transcript level (UniProtKB, Isoforms P29530 and P29531 23−24 kDa; C3VHQ8, 17−18 kDa; C6SZ13, 15−16 kDa). Hence, the isoelectric point (pI) of soybean oleosomes is not sharp due to slight variations of the amino acid composition and distribution of the hydrophilic part (umbrella) of the different oleosins on their surface.

As already mentioned regarding their impact on coalescence, oil bodies of seeds seem to be the most efficient compared to other natural lipid storage organelles, probably due to the required protection against environmental stress during dormancy and germination. In accordance, soy lecithin gives more stable emulsions than egg lecithin.[14] Nevertheless, the usage of intact oil bodies in food products, food processing, and even cooking (e.g., desserts, instant drinks, salad dressing) has not yet commenced, especially in the western world, whereas egg yolk, cream, and other dairy products are very common in food emulsions. For TAGs and phospholipids (soy lecithin), the two main components of the oil bodies, the situation is reversed: compared to animal fat sources, their usage and popularity is higher. More and more animal fat is replaced by vegetable oil, and soy lecithin is the main emulsifier in processed food, for example in chocolate, bakery products, desserts, margarine, or creams. A more practical approach would be to use entire and intact oleosomes in food systems. One possible explanation for this neglect could be that the interest in oil bodies only quite recently changed from a botanical point of view to possible food applications. In 2007, Iwanaga et al.[15] showed the extraordinary stability of oil bodies against heat (90 °C), pH and salt concentrations in the bulk. Chen et al.[16] recently described the role of oleosomes for the formation of yuba, the "skin" formed on soy liquids. This traditional Asian soybean food product is formed as a film-like structure on the surface of heated soymilk.

Moreover, oleosomes are also attractive for genetic engineering and biotechnology, where they are used as plant expression system for recombinant proteins or peptides, e.g., antibodies or vaccines. The protein−oleosin fusions are enriched in the seed oil bodies, which are easy to harvest via flotation-centrifugation and, after cleavage, eukaryotic proteins without potential contamination of animal pathogens are obtained.[11] In addition, as the oil content of soybeans is around 20%, there is a high amount of oleosomes and oleosins available from soybean crops. Improvements with regards to the yield and the upscaling of the oleosome extraction process are promoted by researchers involved in the aqueous extraction of soybean oil.[17]

In summary, the understanding and controllability of the stability of soybean oleosomes are of interest for various applications, such as in food industry, biotechnology or basic research. Presumably, their beneficial behavior originates from their protective function. Oleosomes are oil bodies and function as lipid storage organelles in plants, e.g., in seeds.[7]

To better understand the nature of the oleosomes, systematic experiments have been performed in this study. First, oleosomes are purified at pH 11 similar to a procedure introduced by Chen and Ono.[18] Subsequently, oleosomes are investigated at the air−water interface of a film balance. This procedure allows studying the stability and the behavior of their three different constituents, i.e., the oleosins, the phospholipids and the TAGs. This method offers two basic types of measurements. First, kinetics are recorded, which show the instability and the "destruction" of the oleosomes at the air−water interface and second, the behavior of the oleosomes and their constituents under two-dimensional pressure is studied. Consequently, we can expect several physical scenarios. Oil bodies immersed in the subphase will rise to the surface. First, some oleosomes may stay intact and agglomerate at the interface. Others break up into a phase of TAGs, phospholipids and oleosins. The oil spreads on the surface as a film or droplets. The phospholipids separate from the oil droplets and either move straight to the air−water interface or form micelles in the subphase. Depending on their concentration and charge state on the surface, oleosins can aggregate or assemble in different conformations and arrangements with the surrounding lipids on the surface (Figure 7). Of course, these processes are influenced by many parameters, such as the pH-value and ionic strength, especially as proteins are involved, since their behavior depends strongly on their charge defined by their amino acids exposed to the aqueous environment.

Thus, when the oleosomes are (partially) destroyed at the air−water interface, four different components with competing interactions determine the physical picture at compression of the barriers of the film balance: TAG's, phospholipids, partially denatured oleosins, and still intact oil bodies, which will have different contributions to the area vs surface pressure relation. Depending on their concentration phospholipids will form different phases at the surface (see for example[19−23]), TAGs will partially wet[24] the interface, and oleosins can arrange in different configurations as shown in Figure 7.

So far, many advances[25−27] have been made to study isolated oleosins but as the purification process is difficult due to the high stability of the oil bodies, detergents[28,29] or chaotropic agents have to be used which might influence the protein structure and conformation and hence, no certain facts could be elucidated. However, the knowledge gained during the research of LDL particles can be of help here. In 2003, Martinet et al.[5] published a study on the "Surface properties of hen egg yolk low-density lipoproteins spread at the air−water interface" to investigate the surface active behavior of low-density lipoproteins and their lipid components to clarify the role of each constituent in the lipoprotein film. This approach may also be used to study the adsorption mechanism and surface organization of oleosomes at the air−water interface which should provide useful information about the otherwise difficult to access oleosins.

The physical scenarios of the suggested oleosome behavior are on the one hand supported by observations on hen egg yolk LDL-particles, as it was studied previously. On the other hand, Bonsegna et al.[30] reported that oil bodies purified from hazelnut and almond seeds exhibited a strong surface-active layer at the air−water interface, increasing the surface pressure to around 15 mN/m (available surface area not given), which is supposedly due to a migration of OB to the interface and the subsequent formation of a surface film. These authors report of a floating 2D film surrounding 3D domains of large and brilliant aggregates, visualized with Brewster angle microscopy, which they attribute to the formation of a fluid phospholipid monolayer, where intact oil bodies or oil body aggregates can be dynamically embedded. Bonsegna et al. conclude that the 3D aggregates coalesce with time and that simultaneously new oil bodies from the bulk of the aqueous subphase are reaching the interface, since the surface pressure remains practically

constant over time at constant surface area. They also claim that the 3D aggregates become progressively larger and brighter.

Brewster angle microscopy (BAM) is therefore the method of choice to visualize areas of different brightness due to a different molecular density and/or refractive index in a thin interfacial layer and has long been used to study, for example, lipids, proteins and mixed systems at the air−water interface.[31−34] This technique is indeed a very useful tool in the characterization of the interfacial behavior of oleosomes as no marking is necessary to visualize them. Also, the surface pressure is recorded simultaneously to the BAM micrographs, so the changes in surface tension can be correlated directly with the surface active components seen by BAM.

In the present paper, oleosomes purified from soybeans have been studied at the air−water interface at different subphase conditions to determine the effects behind oleosome stability. Such investigations are prerequisites to better understand the principal function of oleosins and are additionally of interest for food technological applications or carriers. As oleosins tend to form insoluble protein aggregates after being dissolved from the oil bodies, it would be highly desirable for industrial applications to develop methods that prevent this aggregation after oleosin purification.

MATERIALS AND METHODS

For all preparation steps, ultrapure water, filtered with a Millipore device (Billerica, MA/USA) was used and all experiments were carried out at room temperature.

Oleosome Purification. Isolation of soybean oleosomes was performed by a modified aqueous flotation-centrifugation method proposed by Chen and Ono.[17] Dried soybeans (Davert GmbH) were soaked in deionized water at 4 °C for at least 20 h. Then water was added to obtain a 10% soybean-to-water ratio, which was grounded in a Vorwerk Thermomix TM31 at highest speed (10,200 rpm) for 90 s. The resulting slurry was filtered through two layers of Kimtech science precision wipes 21 × 11 cm (Kimberly Clark) to obtain raw soymilk. 25% Sucrose (w/w) was added to the raw soymilk and the pH was adjusted to 11.0 with 1 mol/L NaOH (AVS Titrinorm, Prolabo/VWR) solution. The solution was filled into six 50 mL centrifuge tubes (Roth), which were centrifuged in a Thermo Heraeus Multifuge X1R with 15000xg at 4 °C for at least 5 h. The resulting floating fractions (creamlayer, fat pat, oleosomes) were lifted with a small spoon and resuspended in 45 mL of 20% (w/w) sucrose in deionized water (pH 11) in a new centrifuge tube. After anew centrifugation (15000xg, 4 °C, 5 h), this washing step was repeated once more. The resulting oleosomes were collected and dispersed in 20 mL of deionized water and dialyzed overnight with Thermo Scientific Slide-A-Lyzer G2 Dialysis Cassettes (20K MWCO). The final oleosome emulsion had a water content of 86−88%.

Sodium Dodecyl Sulfate−Polyacrylamide Gel Electrophoresis (SDS-PAGE). The SDS-PAGE was performed with the invitrogen NuPAGE-System. NuPAGE MES-Running Buffer and a 10% NuPAGE Novex Bis-Tris Mini Gel were applied according to the manufacturer's instructions but without heating the samples (diluted dialyzed oleosomes). Instead, they were solubilized overnight at room temperature with the NuPageLDS Sample Buffer and the NuPageLDS Reducing Agent. Further defatting of the samples was not necessary.

For the visualization of the protein bands Coomassie G-250 SimplyBlue SafeStain (invitrogen) was used. After staining for 1 h, the polyacrylamide gel was destained twice with ultrapure water for 1 h and subsequently overnight.

Buffer. For buffered subphases, the following chemicals were used: Phosphoric acid, ACS reagent, (Sigma-Aldrich, Munich/Germany, ≥85 wt % in H_2O), acetic acid (Sigma-Aldrich, Munich/Germany, ≥99.8%), monosodium phosphate (Fluka, Munich/Germany, ≥99%), MES/2-(*N*-morpholino)-ethanesulfonic acid (Carl Roth, Karlsruhe/Germany ≥99%) and Tris/Tris(hydroxymethyl)-aminomethane (Sigma-Aldrich, Steinheim/Germany, 99+%). For varying the ionic strength, the molarity of the buffer was kept constant and the required amount of sodium chloride (Prolabo/VWR, Darmstadt/Germany min. 99.5%) was added.

Film Balance. The surface pressure was measured as a function of time (Kinetics) and surface area (Isotherms) on a Nima (Biolin Scientific, Västra Frölunda/Sweden) BAM Trough (available area at completely opened barriers = 715 cm^2), with symmetric Delrin twin barriers. The trough was equipped with a surface pressure sensor that uses the Wilhelmy plate technique to determine the change in surface tension of the air−water interface in the presence of surfactant molecules. In general, measurements were repeated at least 3 times for any given set of parameters with a very good agreement between the different measurements.

Kinetics. The surface pressure was recorded as a function of time at maximum surface area. Different oleosome concentrations were inserted into the subphase with a pipet (Eppendorf, Hamburg/Germany). Preliminary experiments have shown that no agitation was necessary to enable proper mixing of oleosomes in the subphase. The total volume of the trough was 500 mL.

Isotherms. Immediately after oleosome injection or subsequently to a kinetic measurement, the surface pressure was recorded as a function of area, hence monitoring the changes in surface tension upon compressing. The barrier compression speed was 30 cm^2/min.

Brewster Angle Microscopy. All BAM micrographs were taken on a EP^3−BAM (Nanofilm, Göttingen/Germany) with a lateral resolution of around 1 μm. The size of the micrographs was 600 × 500 μm^2 and images were not processed in any way except for background correction carried out with the provided software. Simultaneously, the surface pressure was recorded.

RESULTS AND DISCUSSION

Oleosome Purification and Characterization. The dialyzed oleosomes had a water content of 86−88%. Their mean diameter of 300−350 nm was measured by means of Dynamic Light Scattering (DLS), at room temperature and diluted in water, with a Nicomp particle sizer (model 380, PSS, Santa Barbara, CA) at a scattering angle of 90° (data not shown). The Coomassie stained SDS−PAGE (Figure 1) confirmed three proteins of 15−16, 17−18, and 23−24 kDa corresponding to approximately the size of the four soybean oleosins known in protein databases (UniProtKB, Isoforms P29530 and P29531 23−24 kDa; C3VHQ8, 17−18 kDa; C6SZ13, 15−16 kDa), when compared to the molecular weight marker (SeeBlue Plus2 Pre-Stained Standard, Invitrogen).

This confirms that pH 11 extraction removed the unspecific bounded soybean storage proteins (glycinin and β-conglycinin), and further potentially allergenic proteins (such as Gly m Bd 30K)[14] from the surface of the oleosomes as shown in the

dx.doi.org/10.1021/jp211871v | J. Phys. Chem. B 2012, 116, 10832−10841

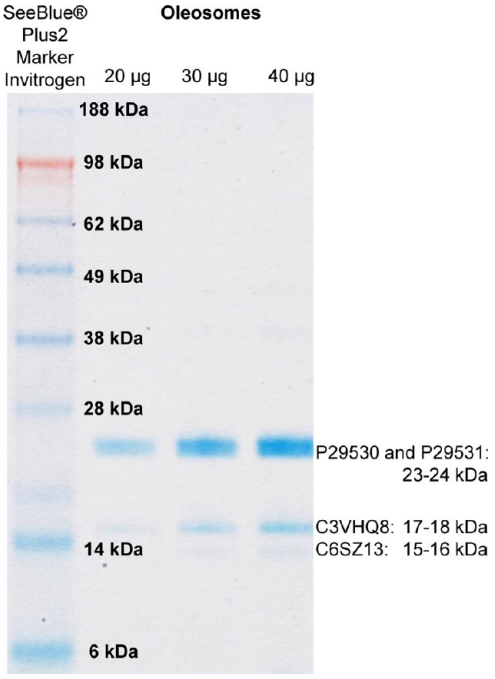

Figure 1. Coomassie-stained SDS–PAGE gel of purified and dialyzed soybean oleosomes in different quantities (20, 30, and 40 μg). Before loading the oleosome samples on the gel, they were solubilized with the NuPageLDS Sample Buffer and the NuPageLDS Reducing Agent overnight at room temperature.

SDS–PAGE. Compared to other oleosome purifications,[12] the oleosomes used here showed a very sharp aggregation behavior between pH 4.4 and 5.7 (data not shown).

Film Balance. Immediately after oleosome injection, the surface pressure increases from 0 mN/m to approximately 12 mN/m (Figure 2). Simultaneous BAM micrographs during these first seconds show a diffusion of round, very bright 3D particles in the size of the lateral resolution (approx. 1 μm) of the Brewster angle microscope to the air–water interface, presumably oleosomes (Figure 2C). This diffusion decelerates within the first minutes. This initial increase in surface pressure is independent of the subphase conditions but this is not the case for the following progression, which depends strongly on the oleosome concentration, pH and ionic strength of the subphase.

Oleosome Concentration. Surface pressure as a function of time with systematic variation of oleosome concentration is shown in Figure 2, revealing two different cases of surface pressure trends over time. At low concentrations ($\leq$0.4 mg/L), the surface pressure vs time shows a maximum, whereas at high concentrations ($\geq$0.8 mg/L), a slow but constant rise in surface pressure with time is observed. Apparently, between the concentration of 0.4 and 0.8 mg/L the behavior of the surface film changes drastically. Hence, 0.4 and 0.8 mg/L oleosome concentrations are discussed exemplarily for the two different scenarios of soybean oleosome behavior at the air–water interface:

When oleosomes of 0.4 mg/L concentration are added to the subphase, an initial steep rise of surface pressure up to 12 mN/m can be monitored and simultaneous BAM micrographs show round objects with a few micrometers in diameter at the air–water interface, presumably oleosomes. After this initial increase, the surface pressure increase flattens and the number of observed interfacial oleosomes decreases until a maximum pressure of approximately 16 mN/m is reached. This is the first indication of a rupture of the oleosomes during the rise of the surface pressure as this would lead to more components at the interface and subsequently higher surface pressures. When the pressure decreases beyond the maximum of the peak, no more oleosomes are observed by BAM, which further strengthens the rupture hypothesis. This decrease in surface pressure can be explained by the aggregation and descent of free oleosins and the subsequent formation of domains of free lipids.[35]

The onset of the surface pressure peak may occur at later times, but the described behavior is the same. We suppose this can be correlated with a different lifetime of intact oleosomes at the interface, which is dependent on air humidity, but future investigations are needed to verify this assumption.

For a better understanding of the composition of the interfacial film formed by a 0.4 mg/L oleosome concentration, isotherms were recorded before, on, and after the peak and BAM micrographs were taken (Figure 2C). When the area is decreased by compression before the surface pressure reached its maximum, hence prior to presumptive oleosome rupture, no phase transitions are visible in the isotherm. However, if the film is compressed at the peak of the surface pressure, a transition in the isotherm is observable at 20–25 mN/m, which becomes more pronounced for longer times (175 min compared to 75 min). Additionally, the longer the time between reaching the peak in the kinetic and compression of the film, the more precise the shape of this phase transition will be. This transition is supposedly due to free lipids (which are only available in significant quantities after most of the oleosomes are ruptured) and can get more distinct when lipids start to form domains. The latter is supported by the fact that structures resembling lipid domains are visible in the BAM pictures during the compression of 0.4 mN/m.

For higher concentrations, the same initial steep rise of surface pressure after oleosome injection as for low concentrations can be monitored. However, afterward, the surface pressure continues to rise slowly and BAM micrographs and isotherms are comparable to the ones described in more detail later (Phase Transitions after Different Times).

Figure 2B compares isotherms for these two different cases recorded at a "pseudo-equilibrium" stage after 5 h. For 0.4 mg/L, two phase transition are visible, one at 20–25 mN/m and one around 35 mN/m, while the isotherms of higher concentrations show only the latter around 35 mN/m. Because of the limited pressure range accessible for different concentrations, it is hard to determine whether the lower transition is just outside the accessible surface pressure range or is really not existent for higher concentrations due to a different film composition. However, isotherms at 0.8 mM/m after shorter kinetics as well as the different BAM micrographs recorded at intermediate surface pressures suggest a different film composition and strengthen the hypothesis that the lower transition only occurs for cases where the kinetic shows a maximum in the surface pressure. For the higher concentrations, distinctively different BAM micrographs are recorded during compression, showing structures indicating oleosin aggregates. Also a highly viscous film is formed. Before the isotherm reaches the plateau of 35–40 mN/m this protein film builds up layers which can be pulled out as thin viscoelastic strands at the end of the compression (Figure 2B). The previous phase behavior shows characteristics of a liquid

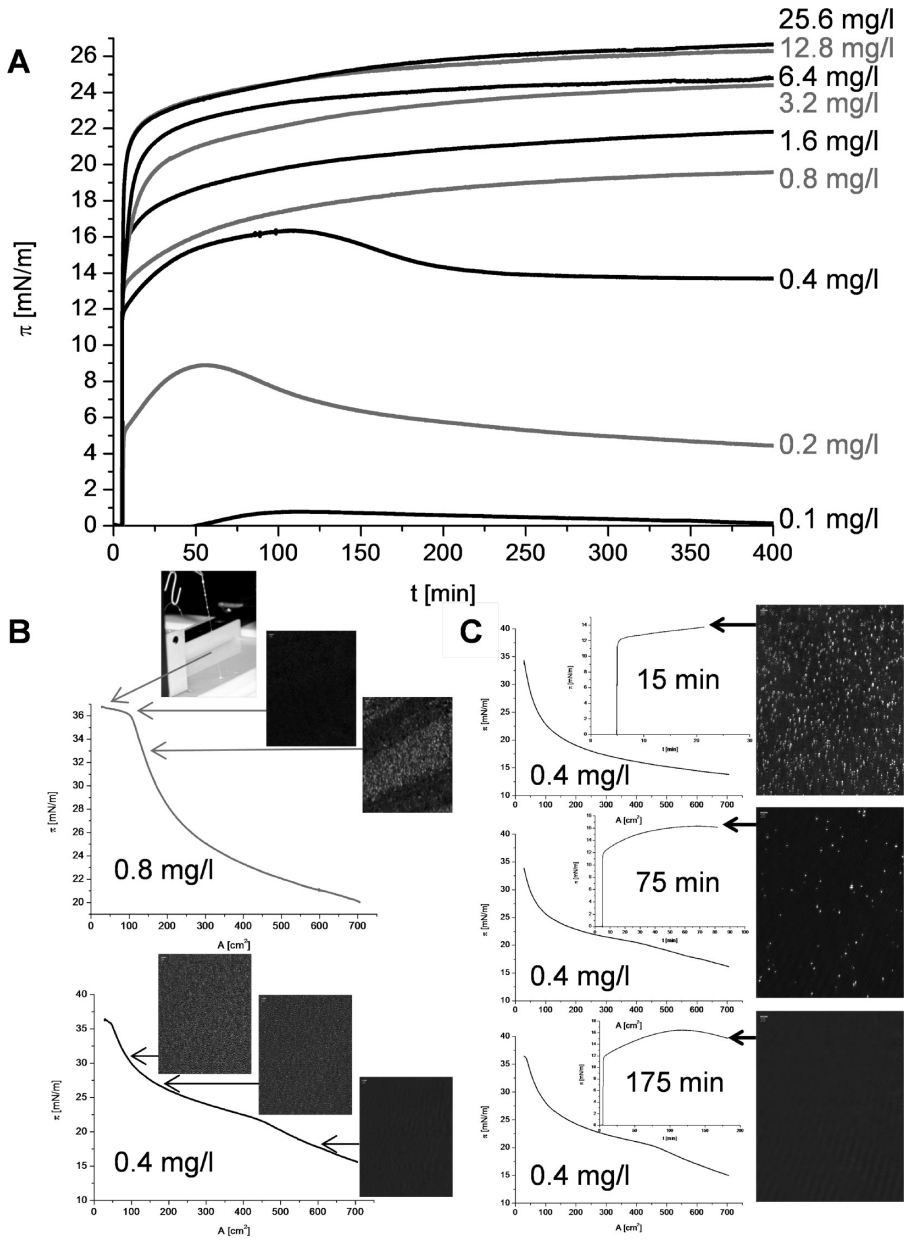

Figure 2. (A) Measurement of surface pressure as a function of time and for increasing oleosome concentrations ranging from 0.1 mg/L to 25.6 mg/L. Surface pressure of 0.1−0.4 mg/L oleosome concentration peaks at different times. Surface pressures of concentrations ≥0.8 mg/L are rising constantly during observation time with a maximum surface pressure of approximately 26 mN/m. (B) Isotherms (v_B = 30 cm²/min) and BAM micrographs of oleosome concentrations 0.4 and 0.8 mg/L after 5 h exhibit phase transitions at 20−25 mN/m and/or 35−40 mN/m. During compression lipid domains are visible in the BAM micrographs. For ≥0.8 mg/L oleosome concentration, aggregates occur and at the end of the compression thin viscoelastic strands can be pulled from the interface. (C) Kinetics and isotherms (v_B = 30 cm²/min) with BAM micrographs before, on, and after the surface pressure maxima indicating the rupture of oleosomes during the ascent and the formation of lipid domains during the descent. Conditions: 5 mM monosodium phosphate, pH 7.0; 3.36 μL (0.1 mg/L) to 859 μL (25.6 mg/L) of a 14902 mg/L dilution was introduced into the subphase of 500 mL.

expanded/liquid condensed coexistence[36] (LE/LC) of phospholipids.

Those observations let us assume that after oleosome injection, a two-step process takes place:

First, oleosomes diffuse to the air−water interface due to buoyant force, visible in the fast motion of very small objects and the increase in surface pressure. Bursting of oleosomes, which is faster for higher concentrations, results in further increase of surface pressure and a film of free lipids. After the peak, the formation of domains decreases the surface pressure, and if compressed, a clear phase transition and domains, very alike to phospholipid phase behavior during compression, can be observed. At low concentrations, no oleosin aggregates are visible in the BAM micrographs; presumably oleosins are soluble at the interface and/or in remaining lipid domains.

If, at the beginning, a bigger amount of oil bodies (≥0.8 mg/L) was added to the subphase than can be accommodated at the interface, oleosomes will follow when space gets available by domain formation or removal of oleosins to the subphase. This explains that the surface pressure is not decreasing with time for systems with higher concentrations of OB injected and aggregates are visible even after 1000 min of

dx.doi.org/10.1021/jp211871v | J. Phys. Chem. B 2012, 116, 10832−10841

waiting time. Additionally, oleosins are forced to aggregate and/or denature and form an interconnected film with the lipids that stays intact for a long time. This film hinders further diffusion of components (leading to larger domains) as well as a further diffusion of oleosin aggregates into the subphase, both resulting in a decrease in surface pressure. After the compression of this film, thin viscoelastic strands can be pulled out of the surface, but only if the oleosome concentration is ≥0.8 mg/L, a sufficient amount of time elapsed before compression (approximately 5 h) and at pH ≥ 5.

The reason for this is easily explainable as for concentrations ≥0.8 mg/L, the behavior of the surface film is strongly influenced by the charge of the oleosins, which is linked to the pH and the ionic strength of the subphase. Also the time before compression plays an important role.

Variation of pH. When the pH of the subphase differs from 5 (the pI of the oleosins) - in basic as well as acidic direction—the behavior after oleosome injection is similar to the one observed at the isoelectric point but the surface pressure, when the plateau stage is reached, is lower (Figure 3A). BAM micrographs after equal waiting time (60 min) after oleosome injection show much smaller particle sizes away from the isoelectric point compared to images made at pH 5 (Figure 3B). In accordance, the compression isotherms show higher area values for the higher surface pressure transition presumably related to a transition from LE to LE/LC region (Figure 3C). This is in very good accordance to the visibly smaller aggregate size as bigger, bulkier particles will lead to higher transition areas.

At subphase pHs away from the isoelectric point, the oleosins repel each other—the further away from pH 5, the stronger the repulsion—and are not able to pack as densely as uncharged oleosomes at pH 5. Thus, less free bindings can be saturated and the resulting surface pressure is lower.

In longtime kinetics for high oleosome concentrations, a second effect can be observed: for pH 8 as well as for pH 5 the surface pressure is slightly rising during the whole observation time, whereas for pH 2 the surface pressure peaks and drops afterward. This is correlated to the formation of the network-like film shown in Figure 2B, which occurs for pH 5 and 8, but not for pH 2. In the acidic regime, oleosins seem to be unable to form entanglements, because of a higher net charge. This might be related to the fact that oleosins continue to denature with time and thereby their pI is changed from around 5 to the alkaline regime. This is strengthened by the fact that they are alkaline proteins[10] with a theoretical pI for the soybean oleosins at: 8.02 (P29530), 8.89 (P29531), 7.75 (C3VHQ8) and 9.35 (C6SZ13). Hence, at pH 2 surface active substances might diffuse into the subphase and there is no barrier against phase separation and domain formation of the lipids, leading to a decrease in surface pressure. Digestion of the N- and C-termini of intact oleosomes also inhibits the integration of oleosins into a network-like interfacial film.[35]

Ionic Strength. As mentioned above, the ionic strength I of the subphase also has an effect on the surface active behavior if the oleosomes possess a charge.

At subphase pHs away from the isoelectric point, lower surface pressures are reached at smaller ionic strength at the same waiting times than for higher I. (Figure 4A)

This can be easily explained by the screening length of the salt ions. The higher the ionic strength I the smaller the Debye length ($\kappa \sim (1/I)^{1/2}$) and the better the charge of the oleosomes is screened. If the ionic strength is high enough that all charges are screened, no repulsion occurs and the oleosomes behave similar to uncharged oil bodies at pH 5, resulting in the same surface pressure after 60 min (compare Figure 3A and 4A), bigger aggregates (Figure 4B) and higher transition areas (Figure 4C).

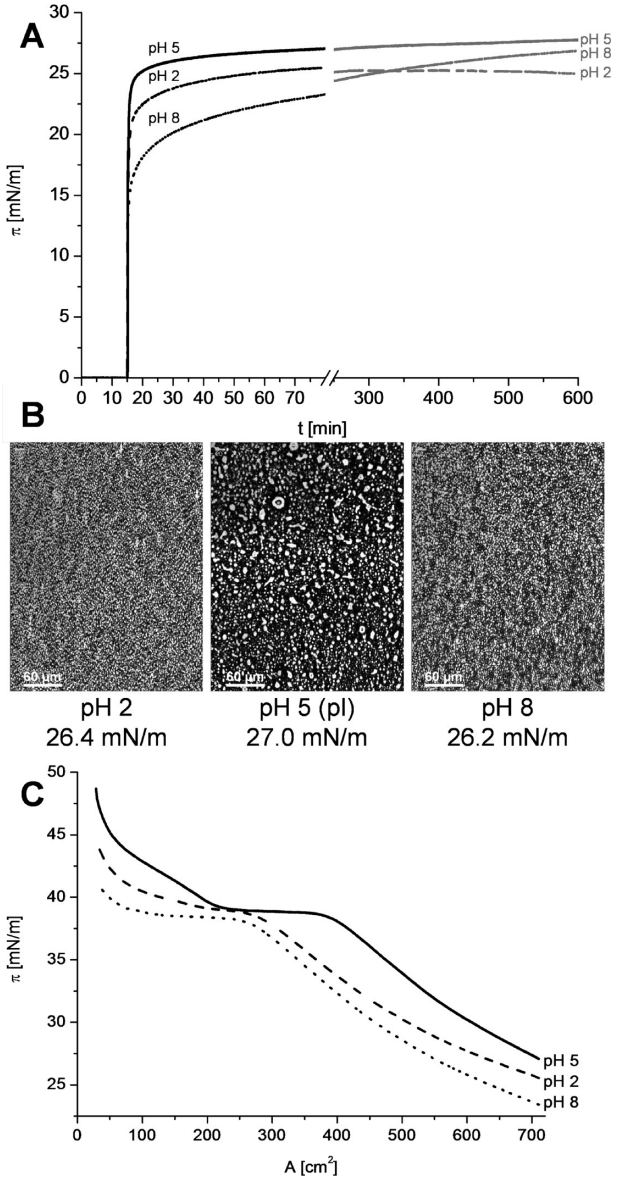

Figure 3. (A) Representative measurement of surface pressure as a function of time at different pH (I = 5 mM). At pH values away from the isoelectric point of oleosomes (pH 5) lower surface pressure values are recorded due to higher repulsion. In longtime kinetics, pH 2 and pH 8 surface pressure curves cross, since at pH 8 (and pH 5), but not at pH 2 a network like film is formed. (B) BAM micrographs at different pH after 60 min, taken at the beginning of the compression. At pH-values away from the isoelectric point, repulsion between the charged oil bodies occurs, leading to smaller aggregates. (C) Compression isotherm at different subphase pH (ν_B = 30 cm²/min, compression after 60 min). For pH values close to the isoelectric point the transition from LE to LE/LC occurs at higher areas. Conditions: 22 μL (6.6 mg/L) OB; pH 2, phosphoric acid; pH 5, acidic acid; pH 8, Tris; all with 5 mM buffer concentration.

Phase Transitions after Different Times. As already mentioned, additionally to pH and ionic strength, the time

dx.doi.org/10.1021/jp211871v | J. Phys. Chem. B 2012, 116, 10832–10841

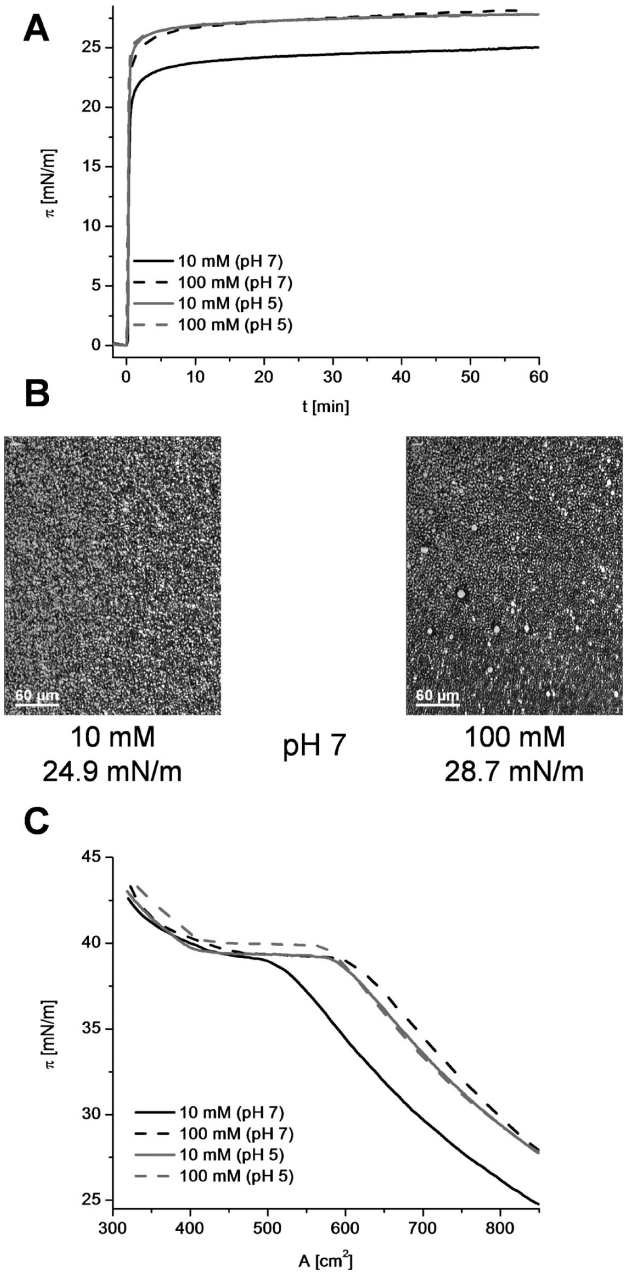

Figure 4. (A) Measurement of surface pressure as a function of time at different ionic strength and pH. Kinetics at pH 5 show no difference in surface pressure if the ionic strength is varied. At pH values away from the isoelectric point, higher ionic strength leads to less repulsion and thus higher surface pressure. (B) BAM micrographs at different ionic strength at pH 7 after 60 min. At pH-values away from the isoelectric point and higher ionic strength, the oleosomes' charge is screened, which induces bigger aggregates. (C) Compression isotherm at different ionic strength and pH (v_B = 30 cm^2/min, compression after 60 min). For higher ionic strength the transition from LE to LE/LC occurs at higher areas. Conditions: 22 μL (5.7 mg/L) OB; pH 5, MES; pH 7, monosodium phosphate; all with 5 mM buffer concentration and ionic strength was adjusted by adding the required amount of NaCl.

elapsing between oleosome injection and compression of the film is crucial for the resulting isotherm.

As shown before, for higher concentrations (≥0.8 mg/L) the surface pressure reaches a plateau stage for long times, where it is not or only slightly increasing (Figure 5A). The particles at the air−water interface are partly aggregating (Figure 5B), leading to bigger structures.

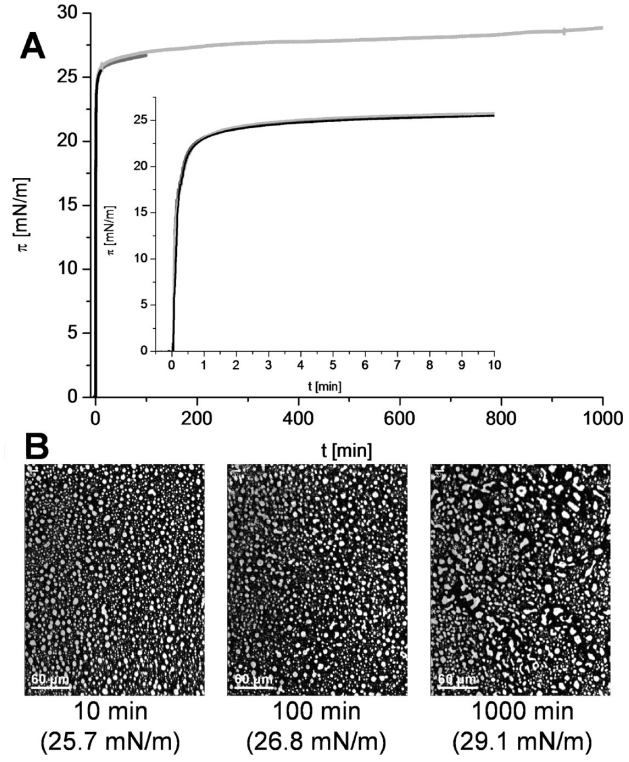

Figure 5. (A) Measurement of surface pressure as a function of time for different durations. The inset shows the first 600 s. (B) BAM micrographs after different waiting times. The longer the waiting time, the bigger are the aggregates. Conditions: 22 μL (5.7 mg/L) OB, 5 mM MES, pH 5.3.

This increase in aggregate size is also reflected in the isotherms. The longer the waiting time between oleosome addition and compression, the higher is the surface area at the LE-to-LE/LC transition and the bigger the plateau of the LE/LC coexistence (Figure 6A).

This can be explained by the bigger and bulkier aggregates which occur at longer waiting times and are forced to interact much earlier during compression than the small round particles that are visible just after injection. Additionally, the surface pressure during the LE/LC coexistence is the lower and elongated the longer the time before compression (Figure 6A). This effect cannot be explained by the growing aggregate size as they also increase in size with increasing ionic strength and at pH close to the isoelectric point were no significant decrease in surface pressure is visible. After approximately 5 h, oleosins seem to form entanglements that result in the network-like film shown in Figure 2B, which might give a preorientation to the phospholipids on the surface and therefore lowers the surface pressure of the LE/LC coexistence. This is observed for pH 5 to pH 8, but more pronounced for pH 5, which is the isoelectric point of soybean oleosomes.

Milli-Q. The events that occur immediately after addition of oleosomes into the subphase proceed very fast and thus focused BAM micrographs are not obtainable (see movie I.avi-LINK).

In the case of not or under-buffered systems those first steps seem to be decelerated and hence can be observed (see movie II.avi-LINK).

This deceleration can probably be attributed to two factors:

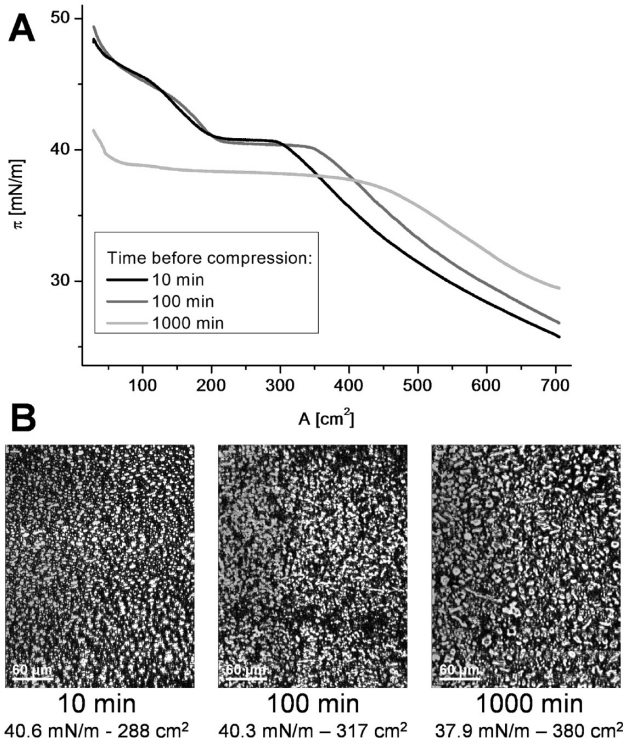

Figure 6. (A) Compression (v_B = 30 cm²/min) isotherm of soybean oleosomes after different waiting times. The longer the waiting time, the higher the area of the LE/LE–LC transition, the longer the LE/LC transition and the lower the surface pressure of this plateau. (B) BAM micrographs after different waiting times during compression. Images are taken at the onset of the plateau stage. Conditions: 22 μL (5.7 mg/L) OB, 5 mM MES, pH 5.3.

- competition for space at the interface
- van der Waals attraction of uncharged oleosomes in buffered systems

The characteristics of the kinetics in unbuffered-water are comparable to the measurements at small oleosome concentrations of around 0.4 mg/L (Figure 2), but in pure water, a higher amount of oleosomes can be used, which raises the chance to observe the "bursting events".

At small ionic strength (approximately below 0.1 mM), after the initial jump to approximately 12 mN/m, the surface pressure is only slowly and linear increasing with time. In this plateau stage, small particles (just above the limit of resolution) start to appear. After a certain amount of time (times scale of minutes), an increase in surface pressure is visible. Brewster angle micrographs during the second increase show an increased fluctuation of the micrometer sized particles, equal to the events after oleosome injection into the buffered subphase but additionally "bursting events" are visible in this stage (see movie III.avi-LINK). Those burstings decrease and disappear as the surface pressure reaches its maximum, according to the hypothesis that at this stage all oleosomes are burst.

CONCLUSIONS

The combination of surface pressure measurements and simultaneous Brewster angle microscopy revealed the oleosome behavior at the air–water interface which is a crucial factor in determining the driving forces in their surface active behavior and the key to using this in practical applications, e.g., food processing. The presumed actions are depicted in Figure 7.

In principle, oleosomes are micelle-like structures with an outer phospholipid monolayer and an interior filled with triglycerides, but with oleosins sticking hairpin-like in the structure with the hydrophilic parts remaining outside the oleosomes.

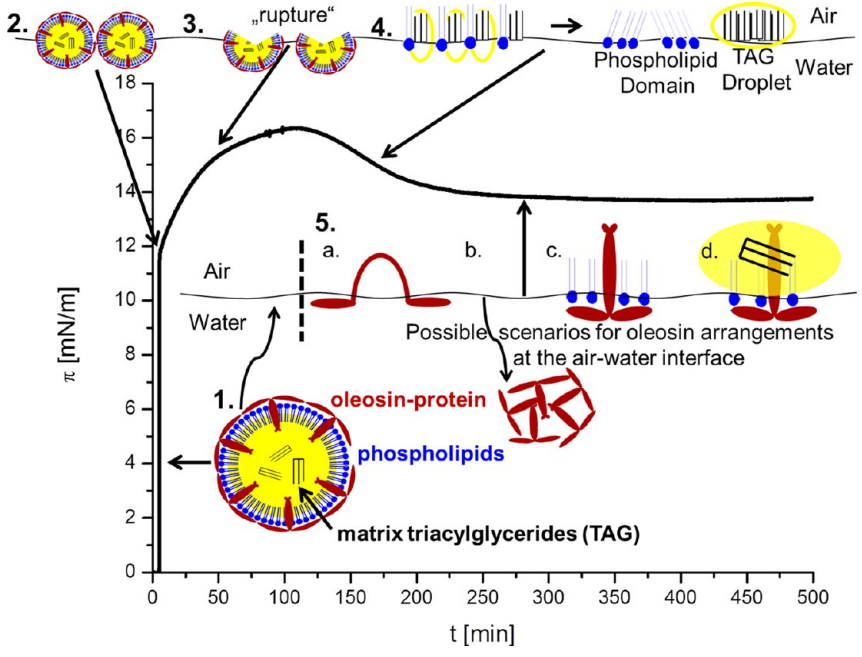

Figure 7. Simplified measurement of surface pressure as a function of time and corresponding scenarios at the air–water interface. The figure shows a typical measurement of the time evolution of the pressure at open barriers for small oleosome concentration (0.4 mg/L). A possible scenario of the oil bodies when exposed to an air–water interface is sketched for illustration (oleosome depiction adapted from Huang[7]).

After injection into the aqueous subphase the oleosomes diffuse immediately to the air−water interface due to their amphiphilic nature and buoyancy, visible in the steep increase in surface pressure and the bright, micrometer sized particles at the air−water interface during this diffusion. At this stage, oleosomes are presumably still intact. Depending on the amount of oleosomes at the surface, bursting of the round structures occurs within different time scales. This rupture can be seen in an additional increase in surface pressure and a decreasing amount of oleosomes visible by BAM. That the rupture is associated with the oil bodies packing at the interface is illustrated in kinetics executed at equal buffer conditions but different amount of oleosomes injected. At low concentrations (≤0.4 mg/L) the surface pressure peaks, whereas at high concentrations (≥0.8 mg/L) a constant rise in surface pressure with time is observed. When the film is compressed soon after an introduction of a small oleosome concentration (≤0.4 mg/L) and before the peak, no kinks are visible in the isotherm as no transitions due to free triglycerides and phospholipids occur. When the film is compressed after rupture of the oleosomes, one to two sharp kinks can be seen. The first, only observable if the initial surface pressure before compression is below 16 mN/m, can probably be attributed to the triglycerides and/or the gaseous/liquid expanded-transition of the phospholipids, which are both able to lower the surface tension after the breakage of the oil bodies. We assume that the second kink is the onset of the liquid expanded/liquid condensed-transition of the phospholipids released from the oleosomes after rupture. Another possible explanation for this kink would be desorption of the oleosin proteins, comparable to the desorption transition of lipopolymers.[37] However, for oleosins, such a behavior seems to be unlikely. First, the strong hydrophobicity suggests an aggregation to micelles, which would be stabilized in the subphase by the two hydrophilic tails of each oleosin. In addition, recent work showed the persistence of this transition after the tryptic digestion of the oleosins,[34] which indicates a phospholipid triggered effect.

The time that elapses during introduction of the oleosomes into the aqueous subphase and rupture depends on the parameters of the subphase, e.g., pH-value and ionic strength as well as amount of oleosomes injected. The denser the packing of the oleosomes at the air−water interface, the faster the rupture.

Additionally, the higher the ionic strength and the closer the pH to the isoelectric point, the higher is the "end surface pressure". This behavior can be explained by the charge of the oleosins. At the isoelectric point, no charges are present and the oleosins do not repel each other, leading to denser packing at the air−water interface and more saturated bindings, thus resulting in higher surface pressure. At higher ionic strength the charges of the oleosins are screened much better, which also results in denser packing at the air−water interface.

Regarding the free oleosins, we propose four possible arrangements:

(a) A denaturation of the oleosins at the air−water interface via unfolding of the hydrophobic hairpin.
(b) A clustering of the hydrophobic parts of several oleosins and possibly diffusion into the bulk after a critical size and weight has been reached.
(c) Insertion of an intact oleosin into a monolayer of phospholipids.[24]
(d) Insertion of an intact oleosin into an oil droplet.

The last two points are strengthened by observations in the literature[27] that oleosin aggregates cannot compete with the high surface activity of the triacylglycerides and phospholipids. The adsorption of oleosins at the interface and its conformational changes will be further investigated by spectroscopic techniques at the air−water and oil−water interface.

The formation of a network like film of protein−lipid complexes[38] with presumably entangled oleosins (pH 5−8, oleosome concentration ≥0.8, ≥5 h time before compression) strongly influences the surface film behavior: it prevents diffusion of surface active substances into the subphase and constrains the mobility of the film, which is of great interest for stabilizing interfaces.

■ ASSOCIATED CONTENT

Ⓦ Web-Enhanced Features

Movies showing events that occur immediately after addition of oleosomes into the subphase (movie I.avi-LINK), the same events for not buffered or under-buffered systems (movie II.avi-LINK), and additional "bursting events" (movie III.avi-LINK),

■ AUTHOR INFORMATION

Corresponding Author

*Telephone: +49 6131 379548. Fax: +49 6131 379100. E-mail: waschatko@mpip-mainz.mpg.de.

Notes

The authors declare no competing financial interest.

■ ACKNOWLEDGMENTS

The authors thank Christine Peter, Mara Jochum, Christoph Globisch, Markus Deserno, Johannes Franz, and Sania Maurer for fruitful discussions, David Baßler, Wanja Wiese, and Torsten Stühn for video editing, and Sandra Ritz for the use of SDS−PAGE equipment.

■ REFERENCES

(1) Griffin, W. C. *J. Soc. Cosmet. Chem.* **1949**, *1*, 311.
(2) Pearce, K. N.; Kinsella, J. E. *J. Agric. Food Chem.* **1978**, *26* (3), 716−723.
(3) Corsi, A.; Milchev, A.; Rostiashvili, V. G.; Vilgis, T. A. *Food Hydrocolloid* **2007**, *21* (5−6), 870−878.
(4) Ettelaie, R.; Akinshina, A.; Maurer, S. *Soft Matter* **2012**, *8* (29), 3582−3597.
(5) Martinet, V.; Saulnier, P.; Beaumal, V.; Courthaudon, J.-L.; Anton, M. *Colloids Surf., B* **2003**, *31*, 185−194.
(6) Patton, S.; Keenan, T. W. *Biochim. Biophys. Acta* **1975**, *415*, 273−309.
(7) Huang, A. H. C. *Annu. Rev. Plant Biol.* **1992**, *43* (1), 177−200.
(8) Hevonoja, T.; Pentikäinen, M. O.; Hyvönen, M. T.; Kovanen, P. T.; Ala-Korpela, M. *Biochim. Biophys. Acta—Mol. Cell Biol. Lipids* **2000**, *1488* (3), 189−210.
(9) Jolivet, P.; Boulard, C.; Beaumal, V.; Chardot, T.; Anton, M. *J. Agric. Food Chem.* **2006**, *54* (12), 4424−4429.
(10) Tzen, J. T. C.; Huang, A. H. C. *J. Cell. Biol.* **1992**, *117* (2), 327−335.
(11) Capuano, F.; Beaudoin, F.; Napier, J. A.; Shewry, P. R. *Biotechnol. Adv.* **2007**, *25* (2), 203−206.
(12) Li, M.; Murphy, D. J.; Lee, K.-H. K.; Wilson, R.; Smith, L. J.; Clark, D. C.; Sung, J.-Y. *J. Biol. Chem.* **2002**, *277* (40), 37888−37895.
(13) Alexander, L.; Sessions, R.; Clarke, A.; Tatham, A.; Shewry, P.; Napier, J. *Planta* **2002**, *214* (4), 546−551.
(14) Palacios, L.; Wang, T. *J. Am. Oil Chem. Soc.* **2005**, *82* (8), 571−578.

(15) Iwanaga, D.; Gray, D. A.; Fisk, I. D.; Decker, E. A.; Weiss, J.; McClements, D. J. *J. Agric. Food Chem.* **2007**, *55* (21), 8711−8716.
(16) Chen, Y.; Yamaguchi, S.; Ono, T. *J. Agric. Food Chem.* **2009**, *57* (9), 3831−3836.
(17) Towa, L.; Kapchie, V.; Hauck, C.; Wang, H.; Murphy, P. *J. Am. Oil Chem. Soc.* **2011**, *88* (5), 733−741.
(18) Chen, Y.; Ono, T. *J. Agric. Food Chem.* **2010**, *58* (12), 7402−7407.
(19) Watkins, J. C. *Biochim. Biophys. Acta—Lipids Lipid Metabolism* **1968**, *152* (2), 293−306.
(20) Blume, A. *Biochim. Biophys. Acta—Biomembr.* **1979**, *557* (1), 32−44.
(21) Albrecht, O.; Gruler, H.; Sackmann, E. *J. Colloid Interface Sci.* **1981**, *79* (2), 319−338.
(22) von Tscharner, V.; McConnell, H. M. *Biophys. J.* **1981**, *36* (2), 409−419.
(23) Möhwald, H. *Annu. Rev. Phys. Chem.* **1990**, *41* (1), 441−476.
(24) Millichip, M.; Tatham, A. S.; Jackson, F.; Griffiths, G.; Shewry, P. R.; Stobart, A. K. *Biochem. J.* **1996**, *314*, 333−337.
(25) Boniewicz-Szmyt, K.; Pogorzelski, S.; Mazurek, A. *Oceanologia* **2007**, *49* (3), 413−437.
(26) Lacey, D. J.; Wellner, N.; Beaudoin, F.; Napier, J. A.; Shewry, P. R. *Biochem. J.* **1998**, *334*, 469−477.
(27) Roux, É.; Baumberger, S.; Axelos, M. A. V.; Chardot, T. *J. Agric. Food Chem.* **2004**, *52* (16), 5245−5249.
(28) Kim, H.; Kim, S.-Y.; Han, N.; Tao, B. *Biotechnol. Bioprocess Eng.* **2007**, *12* (5), 542−547.
(29) Gohon, Y.; Vindigni, J.-D.; Pallier, A.; Wien, F.; Celia, H.; Giuliani, A.; Tribet, C.; Chardot, T.; Briozzo, P. *Biochim. Biophys. Acta—Biomembr.* **2011**, *1808* (3), 706−716.
(30) Bonsegna, S.; Bettini, S.; Pagano, R.; Zacheo, A.; Vergaro, V.; Giovinazzo, G.; Caminati, G.; Leporatti, S.; Valli, L.; Santino, A. *Appl. Biochem. Biotechnol.* **2011**, *163* (6), 792−802.
(31) Beaglehole, D. *Rev. Sci. Instrum.* **1988**, *59* (12), 2557−2559.
(32) Henon, S.; Meunier, J. *Rev. Sci. Instrum.* **1991**, *62* (4), 936−939.
(33) Hoenig, D.; Moebius, D. *J. Phys. Chem.* **1991**, *95* (12), 4590−4592.
(34) Hönig, D.; Möbius, D. *Thin Solid Films* **1992**, *210−211* (Part 1, (0)), 64−68.
(35) Waschatko, G.; Junghans, A.; Vilgis, T. A. *Faraday Discuss.* **2012**, DOI: 10.1039/C2FD20036H.
(36) Kaganer, V. M.; Möhwald, H.; Dutta, P. *Rev. Mod. Phys.* **1999**, *71* (3), 779−819.
(37) Ahrens, H.; Bækmark, T. R.; Merkel, R.; Schmitt, J.; Graf, K.; Raiteri, R.; Helm, C. A. Hydrophilic/Hydrophobic Nanostripes in Lipopolymer Monolayers. *ChemPhysChem* **2000**, *1* (2), 101−106.
(38) Dauphas, S.; Beaumal, V.; Riaublanc, A.; Anton, M. *J. Agric. Food Chem.* **2006**, *54* (10), 3733−3737.